

Connecting Neutron Star Observations to Three-Body Forces in Neutron Matter and to the Nuclear Symmetry Energy

A. W. Steiner^{1,2} and S. Gandolfi³

¹*Joint Institute for Nuclear Astrophysics, National Superconducting Cyclotron Laboratory and the Department of Physics and Astronomy, Michigan State University, East Lansing, MI 48824*

²*Institute for Nuclear Theory, University of Washington, Seattle, WA 98195*

³*Theoretical Division, Los Alamos National Laboratory, Los Alamos, NM 87545*

Using a phenomenological form of the equation of state of neutron matter near the saturation density which has been previously demonstrated to be a good characterization of quantum Monte Carlo simulations, we show that currently available neutron star mass and radius measurements provide a significant constraint on the equation of state of neutron matter. At higher densities we model the equation of state using polytropes and a quark matter model, and we show that our results do not change strongly upon variation of the lower boundary density where these polytropes begin. Neutron star observations offer an important constraint on a coefficient which is directly connected to the strength of the three-body force in neutron matter, and thus some theoretical models of the three-body may be ruled out by currently available astrophysical data. In addition, we obtain an estimate of the symmetry energy of nuclear matter and its slope that can be directly compared to the experiment and other theoretical calculations.

PACS numbers: 26.60.-c, 21.65.Cd, 26.60.Kp, 97.60.Jd

Introduction: While experimental information on matter near the nuclear saturation density is plentiful, there are only a few experimental constraints on matter above the saturation density and, when available, they are contaminated by strong systematic uncertainties. The variation in the energy of nuclear matter with isospin asymmetry is particularly uncertain, since laboratory nuclei probe only nearly isospin-symmetric matter. There is a strong effort in trying to constrain the symmetry energy from intermediate energy heavy-ion collisions [1], giant resonances in nuclei [2], and parity-violating electron-nucleus scattering [3, 4].

Theoretical computations of neutron-rich matter are also difficult, owing to the poor quality of effective forces in dealing with neutron-rich matter [5] and uncertainties in the nature of the three-neutron force. At low densities, neutron matter is well understood because the two-body neutron-neutron interaction is constrained by experimental scattering phase shift data. At higher densities, three different classes of methods have emerged for computing the properties of neutron matter. The first class is based on phenomenological forces like the Skyrme interaction [6]. The second class of calculations is based on microscopic nuclear Hamiltonians that typically include two- and three-body forces obtained from chiral effective field theories, adjusted using renormalization group techniques to do perturbative calculations [7]. However the renormalization of the nuclear Hamiltonian induces many-body forces that have been carefully included in light nuclei [8] but not yet in nuclear matter. An alternative approach is the Brueckner-Hartree-Fock theory, which has been extensively used to study nuclear matter and hyperonic matter [9–11]. The third class uses nuclear potentials, like Argonne and Urbana/Illinois

forces, which reproduce two-body scattering and properties of light nuclei with very high precision [12, 13]. In the latter case, the interaction is designed to have small non-local terms, giving the potentials a hard core. The calculations can be performed in nonperturbative framework, and the strong correlations are solved by using correlated wave functions. The ground state of nuclear systems is determined by using the cluster-expansion [14] or using quantum Monte Carlo (QMC) methods. QMC methods have proven to be a very powerful tool to accurately study properties of light nuclei [15, 16] and nuclear matter [17]. All three of these classes suffer from strong uncertainties above the saturation density, both regarding the method and the nuclear Hamiltonian.

On the other hand, astrophysical observations of neutron star masses and radii probe the equation of state (EOS) of dense, neutron-rich matter above the saturation density. Two types of neutron star mass and radius measurements have provided for progress on constraining the EOS: the measurement of the general relativity-corrected radiation radius of quiescent low-mass x-ray binaries (qLMXBs) [18], and the observation of photospheric radius expansion bursts which provides a simultaneous measurement of both the mass and radius [19–21]. Reference [20] has demonstrated that these two sets of data provide significant constraints on the EOS, ruling out several currently available theoretical models of dense matter.

In this work, we show that these astrophysical observations are beginning to constrain the nature of the three-body force in neutron matter. We construct a phenomenological description of the EOS near the saturation density which faithfully reproduces QMC simulations of neutron matter and can represent a wide range of EOSs

at high density [22, 23]. Utilizing the currently available astrophysical observations, we show that two parameters, closely connected with the strength of the three-body force and related to the magnitude and density dependence of the symmetry energy, are constrained by the observational data.

The model: For densities below about half the saturation density, neutron stars consist of a crust which is solid except for a thin shell at the surface. Since the uncertainty in the EOS of the crust leads to an error in the radius which is much smaller than the current observational uncertainty, we ignore variations in the EOS of the crust (see, e.g., [24]). We use the outer crust from Ref. [25] and the inner crust from Ref. [26]. Near and above the saturation density, we use a parametrization of neutron matter with the form

$$\epsilon_{\text{NM}} = \rho \left[a \left(\frac{\rho}{\rho_0} \right)^\alpha + b \left(\frac{\rho}{\rho_0} \right)^\beta + m_n \right], \quad (1)$$

where ρ is the nucleon number density, m_n is the nucleon mass, and a , α , b and β are free parameters. In Ref. [17, 22] it has been shown that this general form accurately fits the EOS of pure neutron matter given by QMC calculations using realistic nuclear Hamiltonians including two- and three-body forces. The uncertainty of the fit is much smaller than that from the three-body force. In the neutron matter case, the two parameters a and α are mostly related to the nucleon-nucleon force, while the parameter b is mostly sensitive to the corresponding symmetry energy E_{sym} . The parameter β is sensitive to the particular model of three-neutron force (see Ref. [23]). The range of parameters which subsumes all reasonable QMC calculations of neutron matter is $12.7 < a < 13.3$ MeV, $0.48 < \alpha < 0.52$, $1 < b < 5$ MeV and $2.1 < \beta < 2.5$.

Because the parametrization in Eq. 1 describes neutron matter, we must also make a small correction to the neutron matter EOS due to the presence of a small number of protons. In order to estimate this correction, we examine several Skyrme models from Ref. [27], all chosen to have reasonable saturation properties and symmetry energies sufficiently strong as to prevent pure neutron matter from appearing in the maximum mass neutron star. We compute the mean and root-mean-square deviation of the ratio of the pressure of neutron matter to the pressure of neutron star matter as a function of energy density over all the Skyrme models in our set. In our fiducial model, we apply a randomly distributed correction to the pressure with the same mean and root-mean-square deviation as that obtained in the Skyrme models, to our neutron matter EOS. This correction is 0.86 ± 0.03 at saturation density. For comparison, we also repeat our analysis without including the uncertainty in the ratio of the pressures, simply applying the mean correction estimated from the Skyrme models. We have also

checked this correction is similar to that given by similar relativistic mean-field models.

Above the saturation density, four-body forces, hyperons, Bose condensates, and quark degrees of freedom may contribute to the EOS and our parametrization will no longer be appropriate. We take $\rho_t = 0.40 \text{ fm}^{-3}$ as a reasonable upper limit for our parametrization of neutron-rich matter. Our fiducial model describes matter at higher densities by using a sequence of two piecewise-continuous polytropes, $P = \epsilon^{1+1/n}$ with polytropic index n . The three parameters which describe the high-density EOS are n_1 and n_2 , the indices of the two polytropes and ϵ_P , the transition energy density between the two polytropes. Similar parametrizations have been used to describe the EOS at high densities and can mimic the presence of phase transitions.

Alternatively, we describe matter at high densities with a parametrization of quark matter, with a polytrope at moderate densities to represent the possible presence of a mixed phase. For the quarks we use the model proposed by Alford et al. [28]:

$$P = \frac{3a_4}{4\pi^2} \mu^4 - \frac{3a_2}{4\pi^2} \mu^2 - B, \quad (2)$$

where P is the pressure, μ is the quark chemical potential, the coefficient $0.6 < a_4 < 1$ describes corrections to the massless free Fermi gas contribution from strong interactions, the coefficient $a_2 = m_s^2 - 4\Delta^2$ subsumes corrections from quark masses and color superconductivity, and B is the bag constant. A largest possible range for a_2 is between $(150 \text{ MeV})^2 - 4(200 \text{ MeV})^2$ which corresponds to a bare strange quark with a large quark gap and $(400 \text{ MeV})^2$, which corresponds to a zero gap and strange quarks which receive significant contributions from chiral symmetry breaking. This gives four parameters for the high-density part: the index of the polytrope, a_2 , a_4 , and the transition energy density between the polytrope and quark matter which fixes the bag constant B .

To match our parametrization to the constraints from neutron star mass and radius measurements, we use the method outlined in Ref. [20]. To that original data set we add a recent measurement from the transiently accreting neutron star U24 [29]. We also add the constraint that models must be able to support at least a 1.93 solar mass neutron star, consistent with the $1 - \sigma$ lower limit from Ref. [30]. We use Bayesian analysis, taking a uniform prior distribution for EOS parameters and using marginal estimation to compute the posterior probability distribution for EOS parameters, the EOS, and the mass versus radius curve.

Results and discussion: Our constraints on the parameters b and β for the neutron matter EOS near the saturation density are given in Fig. 1, and the parametrization of the high-density part of the EOS is presented as Supplemental material [31]. We find that the posterior

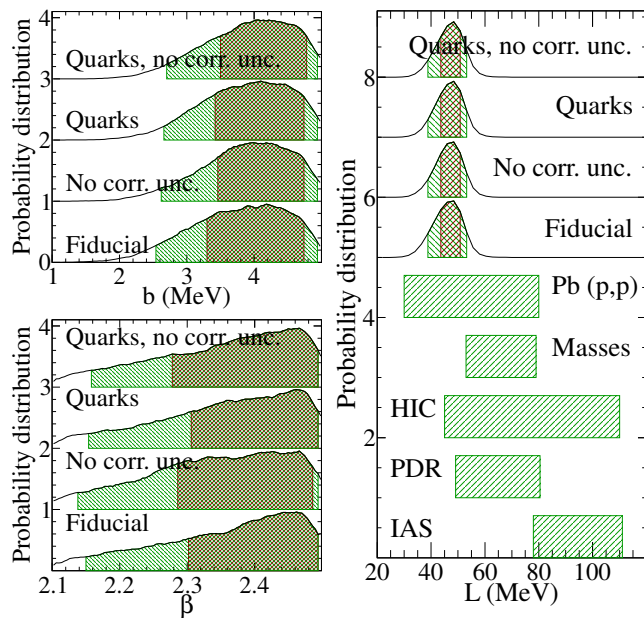


FIG. 1. (Color online) The probability distributions and 68% (dark red areas) and 95% (green areas) confidence ranges for the parameters b and β , and the density derivative of the symmetry energy, L . All distributions have been rescaled so that their peak is unity and then vertically shifted by an arbitrary amount. We compare our predicted value of L with constraints from nuclear masses (“Masses”) [32], heavy ion collisions (“HIC”) [1], pygmy dipole resonances (“PDR”) [2], isobaric analog states in nuclei (“IAS”) [33], and antiprotonic atoms (“Pb(p,p)”) [34]. The parametrization of the high-density part of the EOS is presented as Supplemental material [31].

probability distributions for the parameters a and α associated with the two-body force are almost flat as expected because they are related to the low-density part of the EOS. However, the parameters b and β are strongly constrained by observations to ranges $3.3 < b < 4.8$ MeV and $2.28 < \beta < 2.5$, independent of the nature of the high-density EOS. The results labeled “no corr. unc.” contain no correction for the uncertainty in the ratio of the pressures of neutron matter to neutron star matter in each panel and are nearly indistinguishable from the results where this uncertainty is included (and as a result we always include this uncertainty in the results shown below). We have also checked that the effect of the varying the matching density the neutron matter EOS of Eq. 1 with the polytrope between $\rho_t = 0.32 \text{ fm}^{-3}$ and 0.48 fm^{-3} is small.

Taking the nuclear matter binding energy at saturation to be -16 MeV, the nuclear symmetry energy is $E_{\text{sym}} = 16 \text{ MeV} + a + b$. The density derivative of the symmetry energy, $L \equiv 3\rho_0(dE_{\text{sym}}/d\rho)_{\rho_0}$ is

$$L = 3(a + b) \quad (3)$$

Taking the parameter ranges for a and b showed in Fig.

1 we find $32 < E_{\text{sym}} < 34$ MeV and $43 < L < 52$ MeV to within 68% confidence. These tight constraints are possible because of an interplay between the strong correlation in QMC calculations of neutron matter between E_{sym} and L and the constraints on the EOS from neutron star radii. The correlation between E_{sym} and L results from a separation between short- and long-distance parts of the three-neutron force [23]. Neutron star mass and radius measurements imply the radius is nearly independent of mass and relatively small, which tends to select a smaller value for L and the value for E_{sym} is then constrained from the correlation. We also find that the two- and three-body forces contribute almost equally to the symmetry energy at the saturation density, but this demarcation is more model dependent. Finally, our constraints on the neutron matter EOS are consistent with and complimentary to those from heavy-ion collisions [35], which principally probe symmetric matter.

The various models of three-body forces in neutron matter, that are typically constrained in light nuclei [13], and the fact that the ranges of b and β are nearly independent of the high density EOS implies that neutron star mass and radius measurements can also constrain three-neutron forces. The ranges for b and β are smaller than the constraints determined from the wide range of possible three-body forces given in Ref. [23], demonstrating that the astrophysical observations are ruling out more extreme models for the three-neutron force. The corresponding EOSs are given in Fig. 2 along with the EOS of Akmal, Pandharipande, and Ravenhall (APR) [14] and Skyrme model SLy4 [36]. The solid lines show the limits obtained by Gandolfi, Carlson, and Reddy (GCR) in Ref. [23], obtained without any constraints from neutron star observations.

In Fig. 3, we show the probability of the mass of neutron stars as a function of the radius for the different models. The quark models have slightly larger radii and slightly smaller maximum masses, but the general trend is similar to that described in Ref. [20]. Neutron star radii lie between about 11 and 12.3 km regardless of mass to within 68% confidence. As well as being consistent with QMC calculations from Ref. [23] these results are also consistent with the recent analysis of the EOS of neutron matter using chiral effective theories in Ref. [37].

Finally, we show the pressure of neutron star matter as a function of the energy density in Fig. 4. The results from APR [14], Sly4 [36] and GCR [23]. The quark matter EOS is slightly softer at higher energy densities, but these energy densities are often beyond the central density of the maximum mass neutron star. The pressure in APR is a bit larger than the observations suggest [20], as is clear also in Fig. 2. We stress that any EOS outside the results presented in Figs. 2 and 4, like APR at large energy densities, do not support constraints given by neutron star observations (see also Ref. [20]).

Conclusions: We find that neutron star mass and ra-

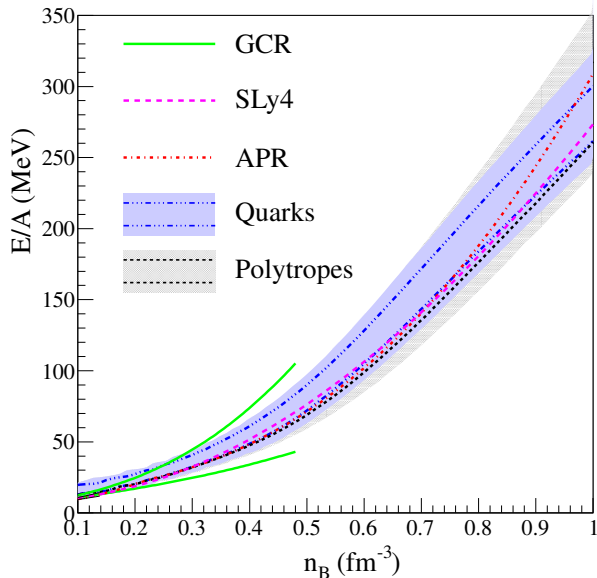


FIG. 2. (Color online) The 68% (dashed and dot-dashed lines) and 95% (shaded areas) confidence ranges for the energy per baryon as a function of the baryon density as constrained by the astrophysical observations. The APR [14] and SLy4 [36] EOSs are also plotted, as well as the limits obtained in Ref. [23] (GCR).

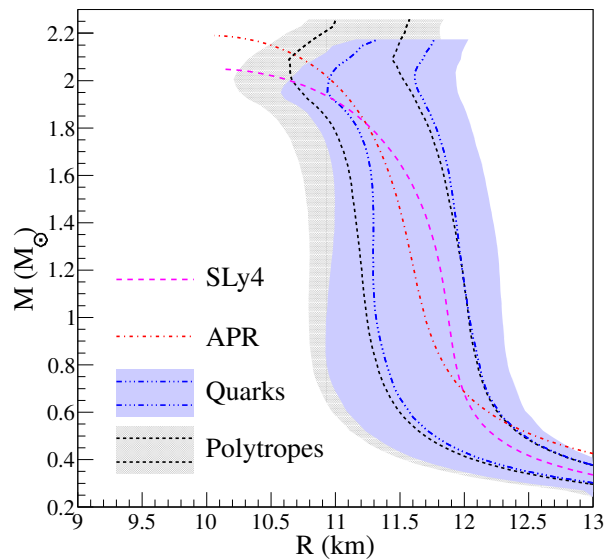


FIG. 3. (Color online) The mass-radius curves for the models considered in this work. The range of radii for 1.4 solar mass neutron stars, between 11 and 12 km, is similar to that obtained in Ref. [20]. The mass-radius curves for APR [14] and SLy4 [36] are also given. The labeling is the same as in Fig. 2.

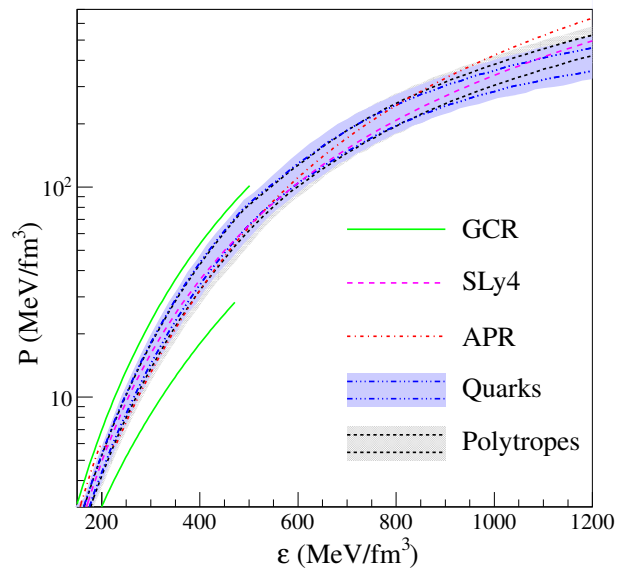


FIG. 4. The pressure as a function of the energy density. The labeling is the same as in Fig. 2.

dius measurements can be used to test and calibrate the three- and many-body nuclear forces in the context of dense infinite matter. In particular we show that, when two- and three-body forces are parametrized as a sum of power-laws in the baryon density, the astrophysical observations strongly constrain both the coefficient and exponent which describes the three-body force. We also find novel constraints on the symmetry energy, driven partially by the strong correlation between S and L obtained in QMC calculations of neutron matter.

There are potential corrections which are not yet well understood, including four-body forces, relativistic corrections, and the possible presence of hyperons [9–11]. Our model partially takes these into account through the high-density polytropes (used above ρ_t) which are not constrained. However, if these corrections are strong below $n_B = 0.32 \text{ fm}^{-3}$, then our constraints will have to be revisited accordingly. Some hyperonic models are consistent with our results [38, 39] while others do not support neutron stars above 1.93 solar masses [10, 11].

Another important difficulty is that there are several potential systematic uncertainties in the neutron star mass and radius measurements which are not yet under control. In the case of the photospheric radius expansion x-ray bursts, these include the nature of the relationship between the Eddington flux and the point at which the photosphere returns to the neutron star surface, the evolution of the spectrum during the tail of the burst [40], a modification of the spectrum due to accretion, and violations of spherical symmetry. In the qLMXBs, the X-ray spectra might contain high-energy power-law features not present in the atmosphere models.

Acknowledgments: We thank J. Carlson and S. Reddy for helpful comments. A.W.S. is supported by Chandra Grant No. TM1-12003X, by the Joint Institute for Nuclear Astrophysics at MSU under NSF PHY Grant No. 08-22648, by NASA ATFP Grant No. NNX08AG76G, and by DOE Grant No. DE-FG02-00ER41132. S.G. is supported by DOE Grants No. DE-FC02-07ER41457 (UNEDF SciDAC) and No. DE-AC52-06NA25396. This work was also supported by the DOE Topical Collaboration “Neutrinos and Nucleosynthesis.”

-
- [1] M. B. Tsang, Y. Zhang, P. Danielewicz, M. Famiano, Z. Li, W. G. Lynch, and A. W. Steiner, *Phys. Rev. Lett.* **102**, 122701 (2009)
- [2] A. Carbone, G. Colo’, A. Bracco, L.-G. Cao, P. F. Bortignon, F. Camera, and O. Wieland, *Phys. Rev. C* **81**, 041301(R) (2010)
- [3] C. J. Horowitz, S. J. Pollock, P. A. Souder, and R. Michaels, *Phys. Rev. C* **63**, 025501 (2001)
- [4] X. Roca-Maza, M. Centelles, X. Viñas, and M. Warda, *Phys. Rev. Lett.* **106**, 252501 (2011)
- [5] S. Gandolfi, J. Carlson, and S. C. Pieper, *Phys. Rev. Lett.* **106**, 012501 (2011)
- [6] J. R. Stone and P.-G. Reinhard, *Prog. Part. Nucl. Phys.* **58**, 587 (2007)
- [7] K. Hebeler and A. Schwenk, *Phys. Rev. C* **82**, 014314 (2010)
- [8] E. D. Jurgenson, P. Navrátil, and R. J. Furnstahl, *Phys. Rev. C* **83**, 034301 (2011)
- [9] Z. H. Li and H.-J. Schulze, *Phys. Rev. C* **78**, 028801 (Aug 2008), <http://link.aps.org/doi/10.1103/PhysRevC.78.028801>
- [10] I. Vidaña, D. Logoteta, C. Providência, A. Polls, and I. Bombaci, *Europhys. Lett.* **941**, 11002 (2011)
- [11] H.-J. Schulze and T. Rijken, *Phys. Rev. C* **84**, 035801 (2011)
- [12] R. B. Wiringa, V. G. J. Stoks, and R. Schiavilla, *Phys. Rev. C* **51**, 38 (1995)
- [13] S. C. Pieper, V. R. Pandharipande, R. B. Wiringa, and J. Carlson, *Phys. Rev. C* **64**, 014001 (2001)
- [14] A. Akmal, V. R. Pandharipande, and D. G. Ravenhall, *Phys. Rev. C* **58**, 1804 (1998)
- [15] B. S. Pudliner, V. R. Pandharipande, J. Carlson, S. C. Pieper, and R. B. Wiringa, *Phys. Rev. C* **56**, 1720 (1997)
- [16] S. C. Pieper, *AIP Conf. Proc.* **1011**, 143 (2008)
- [17] S. Gandolfi, A. Yu Illarionov, S. Fantoni, J. C. Miller, F. Pederiva, and K. E. Schmidt, *Mon. Not. R. Astron. Soc.* **404**, L35 (2010)
- [18] R. E. Rutledge, L. Bildsten, E. F. Brown, G. G. Pavlov, and V. E. Zavlin, *Astrophys. J.* **514**, 945 (1999)
- [19] J. van Paradijs, *Astrophys. J.* **234**, 609 (1979)
- [20] A. W. Steiner, J. M. Lattimer, and E. F. Brown, *Astrophys. J.* **722**, 33 (2010)
- [21] F. Özel, G. Baym, and T. Güver, *Phys. Rev. D* **82**, 101301(R) (2010)
- [22] S. Gandolfi, A. Yu Illarionov, K. E. Schmidt, F. Pederiva, and S. Fantoni, *Phys. Rev. C* **79**, 054005 (2009)
- [23] S. Gandolfi, J. Carlson, and S. Reddy [arXiv:1101.1921](https://arxiv.org/abs/1101.1921) ([*Phys. Rev. C* (to be published)])
- [24] J. M. Lattimer and M. Prakash, *Astrophys. J.* **550**, 426 (2001)
- [25] G. Baym, C. Pethick, and P. Sutherland, *Astrophys. J.* **170**, 299 (1971)
- [26] J. W. Negele and D. Vautherin, *Nucl. Phys. A* **207**, 298 (1973)
- [27] J. Rikowska Stone, J. C. Miller, R. Koncewicz, P. D. Stevenson, and M. R. Strayer, *Phys. Rev. C* **68**, 034324 (2003)
- [28] M. Alford, M. Braby, M. Paris, and S. Reddy, *Astrophys. J.* **629**, 969 (2005)
- [29] S. Guillot, R. E. Rutledge, and E. F. Brown, *Astrophys. J.* **732**, 88 (2011)
- [30] P. B. Demorest, T. Pennucci, S. M. Ransom, M. S. E. Roberts, and J. W. T. Hessels, *Nature* **467**, 1081 (2010)
- [31] See Supplemental Material for the parametrization of the high-density part of the EOS.
- [32] M. Liu, N. Wang, L. Z.-X., and F.-S. Zhang, *Phys. Rev. C* **82**, 064306 (2010)
- [33] P. Danielewicz and J. Lee, *Nucl. Phys. A* **818**, 36 (2009)
- [34] M. Warda, X. Viñas, X. Roca-Maza, and M. Centelles, *Phys. Rev. C* **80**, 024316 (2009)
- [35] P. Danielewicz, R. Lacey, and W. G. Lynch, *Science* **298**, 1592 (2002)
- [36] E. Chabanat, P. Bonche, P. Haensel, J. Meyer, and R. Schaeffer, *Phys. Scr.* **T56**, 231 (1995)
- [37] K. Hebeler, J. M. Lattimer, C. J. Pethick, and A. Schwenk, *Phys. Rev. Lett.* **105**, 161102 (2010)
- [38] I. Bednarek, P. Haensel, J. L. Zdunik, M. Bejger, and R. Mañika [arXiv:1111.6942](https://arxiv.org/abs/1111.6942) (2011)
- [39] S. Weissenborn, D. Chatterjee, and J. Schaffner-Bielich [arXiv:1112.0234](https://arxiv.org/abs/1112.0234) (2011)
- [40] V. Suleimanov, J. Poutanen, M. Revnivtsev, and K. Werner [arXiv:1004.4871](https://arxiv.org/abs/1004.4871) (2011)

SUPPLEMENTAL MATERIAL

In this supplemental material section we provide the parametrization of the high-density part of the EOS described in the paper. The two different parametrizations, using two polytropes or one polytrope and a quark matter model, are presented in Figs. 5 and 6.

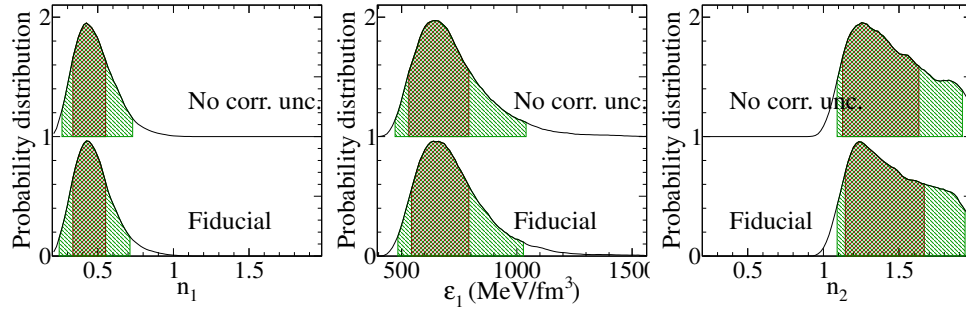


FIG. 5. The probability distributions and 68% (dark red areas) and 95% (green areas) confidence ranges for parameters of the high-density EOS when represented by two polytropes. The polytropic index of the lower-density polytrope is n_1 and the polytropic index of the higher-density polytrope is n_2 . The transition between these polytropes takes place at the energy density specified by ε_1 .

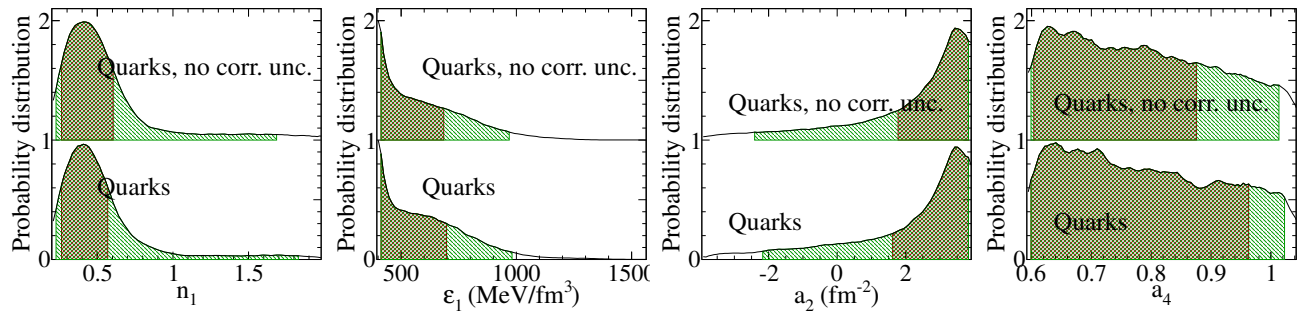


FIG. 6. The probability distributions and 68% (dark red areas) and 95% (green areas) confidence ranges for parameters of the high-density EOS when represented by a polytrope (with index n_1) for the mixed phase and deconfined quark matter at higher densities. The transition between the polytrope and quark matter takes place at the energy density specified by ε_1 . The parameter a_4 and a_2 represent the coefficients proportional to μ^4 and μ^2 in the pressure where μ is the quark chemical potential.